



Commissioning of a radiofrequency quadrupole cooler-buncher for collinear laser spectroscopy

Yin-Shen Liu¹ · Han-Rui Hu¹ · Xiao-Fei Yang¹ · Wen-Cong Mei¹ · Yang-Fan Guo¹ · Zhou Yan¹ · Shao-Jie Chen¹ · Shi-Wei Bai¹ · Shu-Jing Wang¹ · Yong-Chao Liu¹ · Peng Zhang¹ · Dong-Yang Chen¹ · Yan-Lin Ye¹ · Qi-Te Li¹ · Jie Yang² · Stephan Malbrunot-Ettenauer³ · Simon Lechner³ · Carina Kanitz³

Received: 14 February 2025 / Revised: 9 July 2025 / Accepted: 17 July 2025 / Published online: 7 December 2025

© The Author(s), under exclusive licence to China Science Publishing & Media Ltd. (Science Press), Shanghai Institute of Applied Physics, the Chinese Academy of Sciences, Chinese Nuclear Society 2025

Abstract

A RadioFrequency Quadrupole (RFQ) cooler-buncher system was developed and implemented in a collinear laser spectroscopy setup. This system converts a continuous ion beam into short bunches while enhancing the beam quality and reducing the energy spread. The functionality of the RFQ cooler buncher was verified through offline tests with stable rubidium and indium beams delivered from a surface ion source and a laser ablation ion source, respectively. Bunched ion beams with a full width at half maximum of approximately 2 μ s in the time-of-flight spectrum were successfully achieved with a transmission efficiency exceeding 60%. The implementation of the RFQ cooler-buncher system also significantly improved the overall transmission efficiency of the collinear laser spectroscopy setup.

Keywords Radiofrequency quadrupole cooler-buncher · Collinear laser spectroscopy · Hyperfine structure · Time of flight

1 Introduction

The fundamental properties of atomic nuclei, such as masses, nuclear spins, electromagnetic moments, and charge radii, are crucial for exploring exotic nuclear structures and

probing underlying nucleon-nucleon interactions [1–5]. Laser spectroscopy techniques enable the precise determination of the electromagnetic properties of the ground and long-lived isomeric states of atomic nuclei by measuring the hyperfine structure (HFS) spectra of their atoms, ions, and even molecules. Collinear laser spectroscopy (CLS) [2, 6] is a technique capable of achieving high-resolution HFS spectrum measurements. This is realized by overlapping a fast ion beam (~ 30 keV) with lasers in either collinear or anti-collinear geometry, effectively suppressing the spectral Doppler broadening caused by the energy spread of the ion beam [7].

Two typical approaches are used in CLS to measure the HFS spectrum. The most commonly used one is laser-induced fluorescence (LIF), which employs a continuous-wave narrowband laser to excite atoms or ions from their ground or metastable states to higher excited states, followed by the detection of emitted fluorescence using photomultiplier tubes [8]. However, the experimental sensitivity of this approach is often limited by the high background signals caused by stray laser light. This limitation could be tamed by delivering the ion beam in short bunches, which enables to gate data taking on the ion bunch passage through the laser-beam interaction region. As a result, the

This work was supported by the National Natural Science Foundation of China (Nos.12027809, 12350007), National Key R&D Program of China (Nos. 2022YFA1605100, 2023YFA1606403, and 2023YFE0101600), New Cornerstone Science Foundation through the XPLORER PRIZE. The initial simulation and design studies for the MIRACLS RFQ cooler-buncher utilized and adapted in this work has received funding from the European Research Council (ERC) under the European Union's Horizon 2020 research and innovation program under grant agreement No. 679038.

✉ Xiao-Fei Yang
xiaofei.yang@pku.edu.cn

¹ School of Physics and State Key Laboratory of Nuclear Physics and Technology, Peking University, Beijing 100871, China

² Institute of Modern Physics, Chinese Academy of Sciences, Lanzhou 730000, China

³ Experimental Physics Department, CERN, CH-1211 Geneva 23, Switzerland

signal-to-background ratio can be improved by 3–4 orders of magnitude, as demonstrated in Ref. [9]. Another approach for measuring the HFS spectrum using CLS is resonance ionization spectroscopy (RIS), which utilizes multiple lasers to stepwise excite and then ionize the targeted atoms [10]. By detecting resonantly laser-ionized ions with high efficiency, this approach eliminates the need for photon detection, thereby further improving the overall sensitivity of the CLS [11]. To achieve a high resonance ionization efficiency in this approach, high-power pulsed lasers are indispensable. Consequently, the ion beam must be delivered in bunched mode to ensure proper temporal matching between the laser pulses and the ion beam bunches in the interaction region. An earlier attempt to use continuous ion beams for RIS in CLS resulted in limited efficiency owing to duty cycle losses [12]. Therefore, a bunched ion beam is a precondition for high-resolution and high-sensitivity HFS spectrum measurements using the CLS.

In recent years, we have been working on the development of a CLS setup using both LIF and RIS approaches at Radioactive Ion Beam (RIB) facilities in China [13–15]. The first stage of the setup, based on the LIF approach, was implemented at the Beijing Radioactive Ion Facility (BRIF) of the China Institute of Atomic Energy. The first commissioning experiment successfully measured the HFS spectrum of the radioactive ^{38}K isotope [16]. However, compared to the ~ 50 MHz linewidth of ^{38}K HFS spectrum measured by the COLLAPS experiment at ISOLDE [17], the 150 MHz linewidth of the HFS spectrum achieved at BRIF [16] is significantly broader. This spectral broadening was found to originate from the considerable energy spread (δE) of the ion beam delivered by the BRIF facility [16]. This was evaluated using the Doppler broadening formula as follows:

$$\Gamma_{\text{D}} = \frac{\tilde{\nu}_0 \delta E}{\sqrt{2Emc^2}}, \quad (1)$$

where $\tilde{\nu}_0 = 25293.9 \text{ cm}^{-1}$ denotes the laser wavenumber corresponding to the D1 line of the potassium atomic transition.

The RadioFrequency Quadrupole (RFQ) cooler buncher is a beam manipulation device designed to simultaneously satisfy the aforementioned beam requirements for CLS experiments, namely, a pulsed ion beam with a low energy spread. This technique has been extensively implemented in the worldwide RIB facilities, such as IGISOL [9], ISOLDE [18], NSCL [19], and TRIUMF [20, 21], where it has proven effective in delivering high-quality ion beams for a range of applications.

In this work, we present a detailed commissioning test of a newly installed RFQ cooler-buncher system, which is constructed based on a design [22, 23] by the MIRACLS collaboration [24] at ISOLDE-CERN. This system was tested using a stable Rb ion beam in continuous mode from

a surface ion source, and a stable In ion beam in bunched mode (with a typical bunch width of 100 μs) from a laser ablation ion source. Through a systemic test, the optimal operational parameters of the RFQ cooler-buncher system for the subsequent CLS experiment were identified. Under this condition, the system is capable of providing an ion bunch with a 2- μs temporal width while maintaining 60% overall transmission efficiency through the RFQ system.

2 RFQ cooler-buncher system

Figure 1a presents a detailed schematic of the system, including the offline surface ion source and laser ablation ion source, ion optics, RFQ cooler buncher, as well as its control and HV platform. Monovalent positive ions were produced by the ion source and accelerated to ~ 30 keV [25]. The ion beam was reshaped by an electrostatic quadrupole triplet (QT1) lens for a better beam profile and transmission before injection into the RFQ cooler buncher. The cooler buncher was installed inside a six-way cross at a potential slightly lower than the 30-keV ion beam energy. Inside the cooler buncher, the ions collided with the buffer gas atoms, eventually reaching thermal equilibrium. In this manner, any potentially large energy spread of the incoming ion beam is reduced. Simultaneously, the combined radial RF and axial DC electric fields enable the trapping and accumulation of ions, thereby converting the incoming continuous ion beam into ion bunches with low (longitudinal and transverse) emittance, once released from the cooler buncher. Following extraction, the bunched ion beam is re-accelerated to 30 keV, and its beam profile is optimized by QT optics prior to being directed into the CLS beamline. Two Faraday cups (FCs) were installed both upstream and downstream of the RFQ cooler buncher to evaluate the ion beam transmission. The time structure, namely, the time-of-flight (TOF) spectrum of the bunched ion beam, is recorded by a MagneTOF ion detector and data acquisition (DAQ) system [26].

2.1 Ion source

Two types of offline ion sources are used for the RFQ system test: a newly installed surface ion source that provides a stable ion beam in the continuous mode, and a laser ablation ion source that offers a stable ion beam in the bunched mode. The surface ion source, containing Rb atoms (Heat-Wave Labs, #101139), was mounted on a CF150 flange of a six-way cross, as shown in Fig. 1a. This ion source produced stable ion beams of ^{85}Rb (72.17%) and ^{87}Rb (27.83%). With a heating current of 1.44 A, an ion beam current of approximately 100 pA was measured at FC1 by optimizing the extraction electrode and lens in the ion source chamber, as shown in Fig. 1. It is worth noting that under these

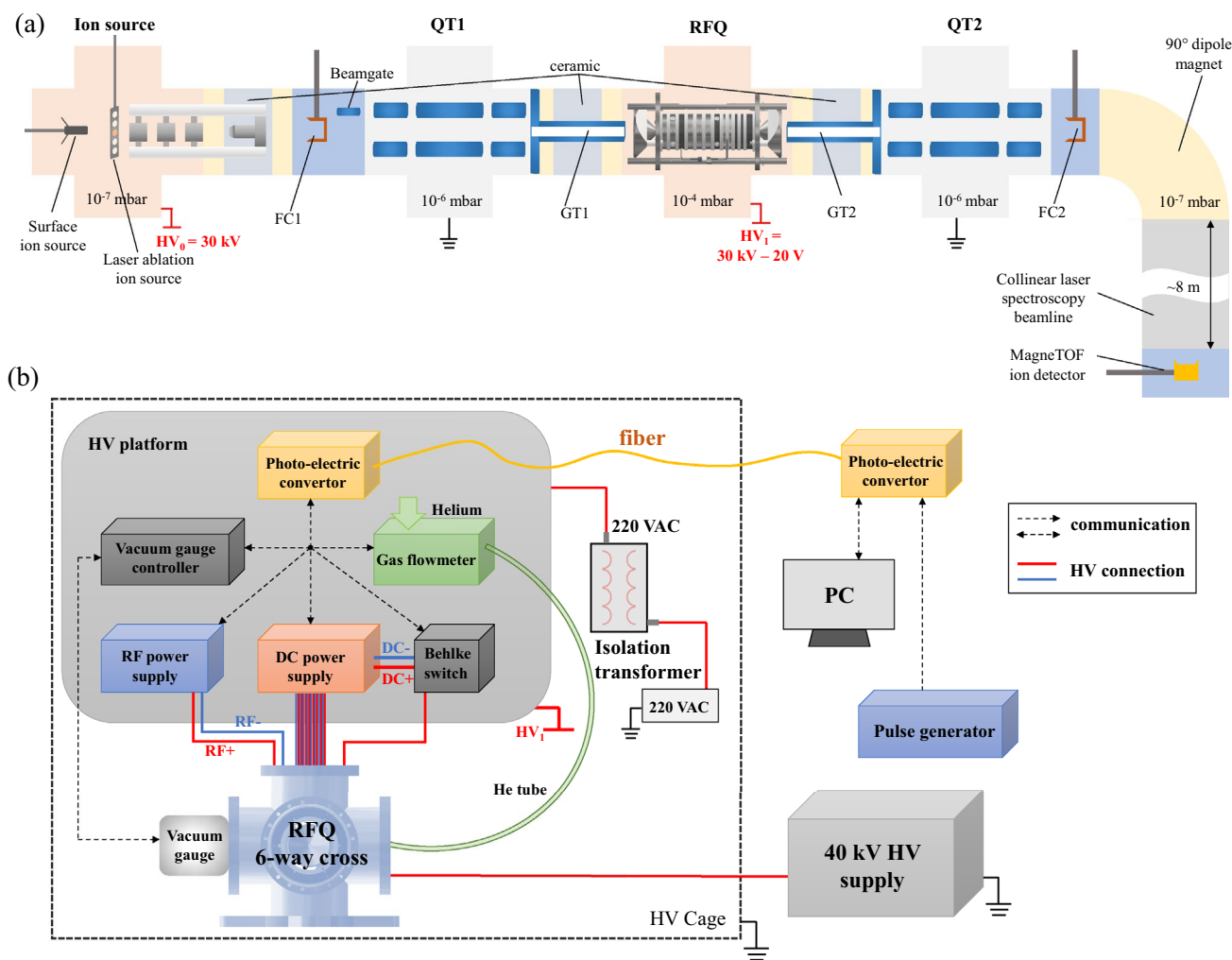


Fig. 1 (Color online) **a** Schematic of the RFQ cooler-buncher system, including the offline surface and laser ablation ion source, ion optics and the RFQ cooler-buncher. QT: Quadrupole Triplet; GT: Ground-

ing Tube; FC: Faraday Cup. **b** Layout of overall control and HV system. See text for more details

conditions, the average fluctuation of the ion beam intensity remains within 1-pA for several hours, which is crucial for the RFQ cooler-buncher test. The details of the laser ablation ion source can be found in Ref. [25]. In brief, an indium target was ablated by a 100 Hz 532-nm Nd:YAG laser (Beamtech Gama-M100) with a power density of 0.2 J/cm² and a pulse width of 10 ns, generating bunched stable indium ion beams with a temporal width of approximately 100 μ s.

2.2 Ion optics and beam diagnose

As shown in Fig. 1a, the stable ion beam, after being extracted from the ion source, was accelerated to ~ 30 keV and monitored directly by FC1. A voltage of -50 V was applied to a grating in front of the cup to suppress secondary electron emissions when the ion beam impinged on the

FC, ensuring accurate beam current reading at the level of 0.1 pA.

The deflector installed after FC1 served as the equivalent beam gate. The voltage applied to the deflector (beamgate) was periodically modulated by an HV switch (Behlke Switch GHTS 30) controlled by a TTL signal. In this manner, the beam current injected into the RFQ cooler buncher can be reduced to below 1 pA, as the ion beam is deflected whenever the beamgate voltage is active. This is to avoid potential space-charge effects inside the RFQ cooler buncher caused by the intense ion beam.

The QT1 lens upstream of the RFQ cooler buncher was designed to ensure efficient transmission during subsequent injection and deceleration processes. A grounding tube (GT1), 150 mm in length and with an inner diameter of 20 mm, is installed inside a ceramic insulator immediately after QT1, which connects the beamline on the ground

potential with the floating vacuum chamber of the RFQ cooler buncher. The purpose of GT1 is to provide a well-defined ground potential for the ions within the insulator tube, ensuring that their trajectory is well-controlled before they are injected into the RFQ cooler buncher. Additionally, this GT1 also functions as a gas flow restricting tube, separating the $\sim 10^{-6}$ mbar vacuum environment in the QT1 region and the $\sim 10^{-4}$ mbar vacuum inside the RFQ cooler-buncher six-way cross. GT2, QT2, and FC2, which are located downstream of the RFQ cooler buncher (Fig. 1a) have identical designs to those upstream, ensuring the optimization of beam quality and evaluation of beam transport. All the aforementioned ion optics and FC are powered by ± 6 -kV HV modules (EHS F0 60n/p) installed in an HV crate (ECH238, iseg company).

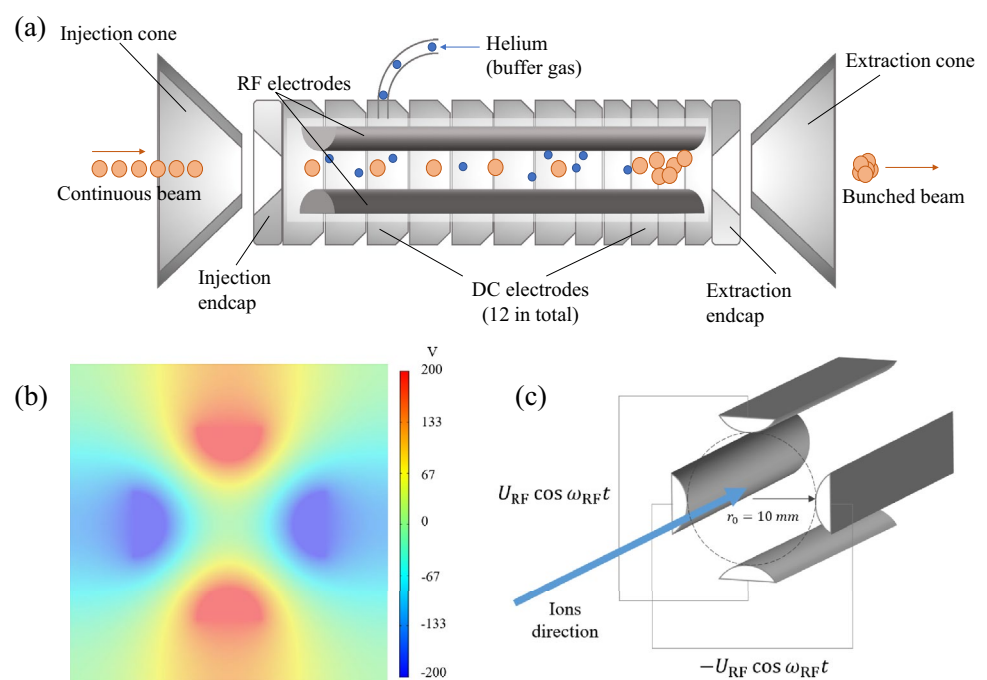
2.3 RFQ cooler-buncher

A comprehensive description about the initial RFQ cooler-buncher's design at MIRACLS will be presented in a forthcoming publication. Here, we describe its implementation and operation as part of the present work. As shown in Fig. 1, the entire RFQ cooler buncher floats above the high potential of HV_1 and is isolated by two ceramic insulators. The internal structure of the cooler buncher is shown in Fig. 2a. The injection section consisted of two electrodes, an injection cone and an injection endcap. The potential of the injection cone was approximately $HV_1 - 2400$ V, while the injection endcap was set to approximately $HV_1 + 13$ V. Both voltages are supplied by ± 6 -kV HV modules (e.g., EHS 80 60n/p) inside a compact HV crate (iseg, ECH224) located on

the HV platform at HV_1 (Fig. 1b). The primary function of these two electrodes, in conjunction with the preceding GT1, is to gradually decelerate the ion beam and guide the ions into the RFQ cooler-buncher via a cone-shaped structure, and detailed simulations of the injection optics can be found in Refs. [22, 27]. Furthermore, the injection endcap features a minimum aperture with a diameter of 5 mm, thereby ensuring a vacuum differential between the inside ($\sim 10^{-2}$ mbar) and outside ($\sim 10^{-4}$ mbar) of the RFQ cooler buncher [27].

Upon entering the cooler buncher, the ions were radially confined by the RF quadrupole electric field (Fig. 2b) generated by the RF electrodes, ensuring optimal ion transmission along the axial direction and trapping with minimal loss. The RF electrodes are composed of four identical semi-cylindrical rods, each with a radius of 5 mm and a length of 152 mm, with a minimum separation of 20 mm between the opposing rods, as shown in Fig. 2c, respectively. The RF power supply (BGTPAX2231, designed and manufactured by Beijing BBEF Science and Technology Co., Ltd.) provides two adjustable sine wave outputs with a frequency range of $f = 0.3 - 1.5$ MHz and an amplitude of $U_{RF} = 0 - 200$ V. These two identical RF signals, except for a 180° phase difference, were applied to two pairs of opposing RF electrodes. Adjacent electrodes were driven 180° out of phase, whereas the opposing electrodes shared the same phase, thereby generating an RF field in the cross-sectional plane of the RFQ electrodes, as illustrated in Fig. 2b: The effective confinement of the radial motion of the ions in the RF field is governed by the Mathieu equation [28], which ensures stability when the parameter $0 \leq q \leq 0.908$, defined as

Fig. 2 (Color online) **a** A schematic diagram depicting the internal structure of the RFQ cooler-buncher. **b** Simulated potential profile of the RF field. **c** Voltages applied to the RF electrodes. Opposite electrodes are driven with voltages of the same polarity, while adjacent electrodes are driven with voltages of opposite polarity. This configuration creates a periodic RF field that confines the radial motion of ions



$$q = \frac{eU_{\text{RF}}}{m\pi^2 f^2 r_0^2}. \quad (2)$$

Here, $r_0 = 10$ mm represents half the distance between opposing RF electrodes.

The energy spread of the ions can be reduced by collisions with the buffer gas atoms inside the cooler buncher during trapping. In our system, helium with a purity of 99.999% was used as the buffer gas. The flow rate of the injected helium gas was adjusted using a flowmeter (Sevenstar, CS200) with a maximum capacity of 100 standard cubic centimeters per minute (SCCM), and the gas was introduced into the cooler buncher via a gas feedthrough on the top flange of the six-way cross. As ions traverse the cooler buncher, they experience continuous collisions with helium atoms. After a brief period (typically 1–5 ms, depending on the ion mass and gas flowrate [22]), ions eventually reach thermal equilibrium with the helium atoms.

The decelerated ions inside the cooler buncher are also influenced by a DC electric field along the axial direction. This electric field, generated by 12 annular DC electrodes positioned along the axial direction, guides the ion beam toward the end section. The first seven electrodes had a thickness of 13 mm, whereas the last five electrodes had a thickness of 8 mm, allowing for more precise electric field control. The potentials of these 12 DC electrodes were supplied by ± 500 V modules (iseg, EBS C0 05), forming an axial electric field together with the extraction endcap electrode. The extraction electrodes mirror those of the injection section; however, the extraction endcap is not directly connected to the HV module. Instead, it interfaces with the HV module via a Behlke Switch (GHTS 30) controlled by a periodic TTL signal. The Behlke Switch features two HV inputs (DC+ and DC-) from ± 6 -kV HV modules (e.g., EHS 80 60n/p) and a single HV output, enabling the application of a periodic voltage to the extraction endcap. During a typical measurement cycle, the control TTL signal for the Behlke Switch remains at a low level, causing it to output a positive DC voltage (e.g. + 1600 V), thereby maintaining a high potential at the end section. Under the combined effects of the RF field, collisions with the buffer gas, and DC trapping potential, ions are gradually cooled and accumulated at the end section. After a sufficient trapping time, the control TTL signal switches to a high level, and the extraction endcap receives a negative voltage (e.g., – 800 V) from the Behlke Switch. Note that the voltage applied to the extraction cone was maintained at a relatively large negative value (e.g., – 2000V) for efficient extraction. As a result, the ions trapped at the end section were released and re-accelerated to nearly 30 keV, eventually forming an ion bunch with a temporal width of only a few microseconds.

To achieve the desired functionality of the RFQ cooler buncher, multiple hardware components are required,

including an RF power supply, a helium gas input, and DC power supplies. All devices associated with this system are illustrated in Fig. 1b: The entire cooler buncher is floated at a high-voltage potential, HV_1 , supplied by a high-precision DC power supply (Heinzinger PNChp 40000-15pos). Consequently, all the associated devices were installed on an HV platform at the same potential, HV_1 , within an HV cage, as shown in Fig. 1b. A 50-kV isolation transformer is employed to electrically isolate HV_1 from the ground potential while supplying 220 VAC power to all the devices on the HV platform. To facilitate remote operation, all devices on the platform were controlled via pairs of photoelectric converters and optical fibers, ensuring bidirectional communication between the control PC and the equipment. This system allows for the control and/or monitoring of key components, such as the RF power supply, DC power supply, gas flowmeter, vacuum gauge controller, and Behlke Switch. The TTL signals required to operate the Behlke Switch were generated using a pulse generator (Quantum Composer 9520).

3 Performance test

The RFQ cooler-buncher system described above was successfully manufactured and installed at Peking University. Because this system will be used to generate bunched ion beams for subsequent collinear resonance laser spectroscopy experiments, our primary focus is on the TOF spectrum width of the ion bunches and the overall transmission efficiency. To evaluate the performance, the bunched ions were detected using a MagneTOF ion detector (ETP, 14924 MagneTOF™ Mini) located downstream in the laser spectroscopy setup, as shown in Fig. 1 of Ref. [29]. The ion bunches generated from the cooler buncher were delivered to the ion detector through a 90° dipole magnet, as depicted in Fig. 1.

Given the large number of parameters involved in the operation of the RFQ cooler-buncher system, a systematic testing approach is required. During commissioning, each component of the RFQ system was individually tested and optimized, followed by iterative fine-tuning of the various device parameters to achieve global optimization. For example, as illustrated in Fig. 3, the influence of the RF parameters and trapping time on the released ion count and TOF width was examined. Using stable Rb ions from the surface ion source, the maximum count rate was achieved with an RF voltage of $U_{\text{RF}} = 167$ V and RF frequency of $f = 500$ kHz, as shown in Fig. 3a. With regard to trapping time, when ions are confined in the RFQ for less than 1ms, the duration is insufficient for effective cooling and trapping, resulting in reduced counts per bunch and a broader TOF width. As the trapping time increased, the released counts per bunch reached a maximum and remained on a plateau within the range of 1–100 ms. Beyond 100 ms, a gradual

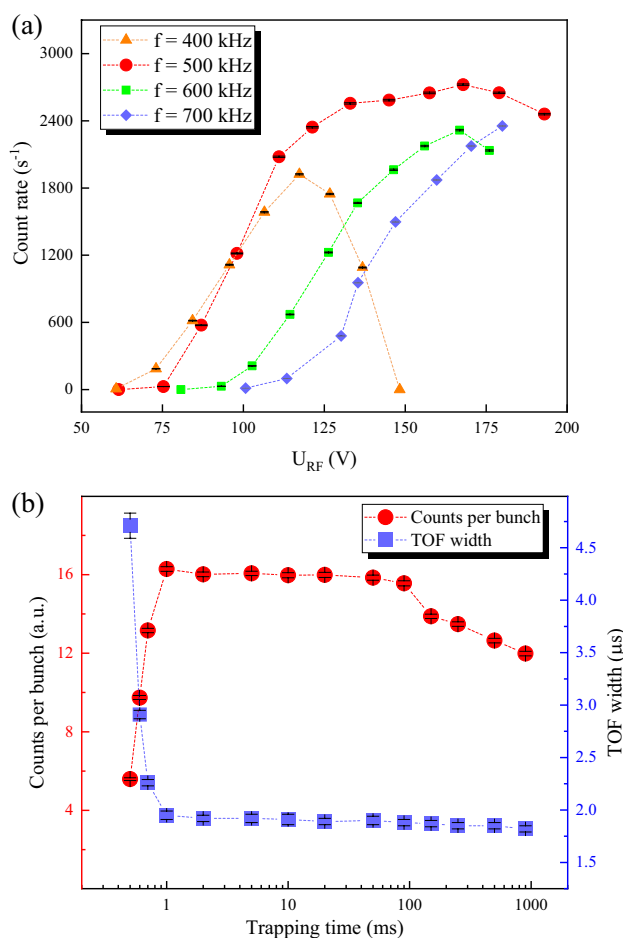


Fig. 3 **a** Count rate of the ⁸⁵Rb ion bunches as a function of the RF voltage amplitude at different RF frequencies. **b** Counts per bunch and TOF width as functions of the RFQ trapping time

decline in counts was observed, suggesting potential ion losses during prolonged confinement. As shown in Fig. 3b, except for a trapping time below 1 ms, the TOF width of the ion bunch remains constant at approximately 2 μs. Taking both the counts per bunch and TOF width into consideration, a trapping time of 5 ms was adopted during commissioning. The RFQ is operated at a repetition rate of 100 Hz to

enable synchronization with the 100 Hz laser pulses used in the subsequent collinear resonance ionization spectroscopy measurement [30].

Other parameters can also influence the properties of bunched ion beams. For example, the DC⁻ and DC⁺ voltages applied to the extraction endcap significantly affect both the ion count rate and TOF spectrum. The potential gradient across the 12 DC electrodes changed the profile of the TOF spectrum (e.g., symmetrical or asymmetrical). The buffer gas flow rate in the range of 10–30 SCCM has only a minor effect on both the ion count rate and TOF width. In principle, a TOF spectrum with a width as narrow as a few tens of nanoseconds can be achieved, as demonstrated by MIRACLS, but this comes at the cost of an increased energy spread and possibly a loss in overall efficiency. However, considering the commonly used TOF width of approximately 2 μs for collinear laser spectroscopy [31, 32], the optimized parameters listed in Table 1 are obtained under conditions that yield an overall RFQ transmission efficiency of 60% for both continuous and bunched modes, as measured using FC1 and FC2. The electrostatic potential along the axial direction of the RFQ cooler buncher calculated using the actual voltage settings listed in Table 1 is shown in Fig. 4. Under these conditions, the observed TOF spectra of ⁸⁵Rb ions from the surface ion source and ¹¹⁵In ions from the laser ablation ion source are shown in Fig. 5. A comparison of the TOF spectra with and without the RFQ cooler-buncher operation clearly demonstrates that this system effectively compresses the continuous ion beam and bunched ion beam with a large temporal width of ~100 μs, narrowing it into significantly narrower ion bunches with a temporal width of ~2 μs, while maintaining an overall efficiency greater than 60%. In addition, the RFQ cooler buncher demonstrated consistent and reliable performance during both this test and the laser spectroscopy experiment [30], operating continuously for 8–10 h per day while providing sustainable beam quality without noticeable degradation. This further confirmed the long-term operational reliability of the RFQ system.

The goal is to integrate the RFQ cooler-buncher system into the collinear resonance laser spectroscopy setup [29] to measure the nuclear properties of unstable nuclei far from

Table 1 A summary of the optimized operating parameters for the RFQ cooler-buncher system, tested with Rubidium ions from the surface ion source

Parameter	Value	Parameter	Value
Element	Rb	DC potential gradient (V/cm)	1.28
Ion source voltage HV ₀ (V)	29986.1	Extraction endcap (release) (V)	HV ₁ – 800
RFQ HV platform voltage HV ₁ (V)	29966.5	Extraction endcap (trapping) (V)	HV ₁ + 1600
Injection cone (V)	HV ₁ – 2400	Extraction cone (V)	HV ₁ – 2000
Injection endcap (V)	HV ₁ – 13	RF amplitude (V)	167
Trapping time (ms)	5	RF frequency (kHz)	500

All values are directly read from the device, except for the DC potential gradient along the axial direction, which is calculated based on the voltages applied to the 12 DC electrodes

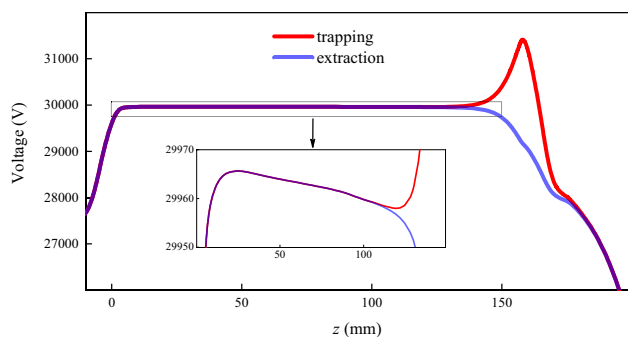


Fig. 4 (Color online) The electrostatic potential along the RFQ axial direction calculated using voltages listed in Table 1. The red line indicates the potential in the trapping mode, while the blue line corresponds to the extraction mode

β -stability on the nuclear chart. However, as discussed in Ref. [29], the earlier test of collinear resonance ionization laser spectroscopy, without the RFQ cooler-buncher system, encountered a major issue: an unacceptable overall ion beam transmission efficiency of less than 40%. This problem primarily arose from the distorted shape of the ion beam delivered into the CLS beamline, which significantly affected the overlap between the ion beam and laser beams within the meter-long interaction region, thereby reducing the resonance ionization efficiency [33]. With the successful integration of the RFQ cooler buncher between the ion source and the laser spectroscopy setup, we achieved an overall ion beam transmission efficiency of >80%, from FC2 to the end section of the CLS beamline, as shown in Fig. 1 of Ref. [29]. This demonstrates that, in addition to producing narrower ion bunches, the RFQ cooler-buncher system also improves the ion beam profile by reducing its transverse emittance,

which is crucial for achieving optimal laser-ion overlapping during the CLS experiment [30]. On this basis, we achieved the high-resolution and high-efficiency HFS spectrum of stable ^{85}Rb , as shown in Fig. 6 (see Ref. [30] for details). These results confirm that the RFQ successfully fulfilled its intended functions for laser spectroscopy experiments.

4 Conclusion and near term experiment plan

In summary, an RFQ cooler-buncher system and its commissioning test are presented. The results demonstrate that this system successfully fulfills its intended functions of compressing the ion beam into short bunches and improving the ion beam profile. With the efficiency of the RFQ cooler buncher exceeds 60%, ion beam bunches with a temporal width of $\sim 2\ \mu\text{s}$ are achieved. Furthermore, the integration of this newly developed system into the offline collinear laser spectroscopy setup significantly improved the overall transmission efficiency of the ion beam owing to the enhanced beam profile with a lower transverse emittance.

Building on these commissioning results, the RFQ cooler-buncher system was first used for the offline test of a collinear resonance ionization laser spectroscopy setup [30]. Soon after, it will be integrated into the online laser spectroscopy experiment of unstable nuclei at the BRIF facility [13] targeting Rb and Cs isotopes. Using a heavy-element target, neutron-rich $^{85-100}\text{Rb}$ and $^{147-150}\text{Cs}$ isotopes have already been produced at the BRIF facility with yields exceeding 100 particles per second. Given the relatively large energy spread of the ion beam at BRIF, approximately 21 eV for

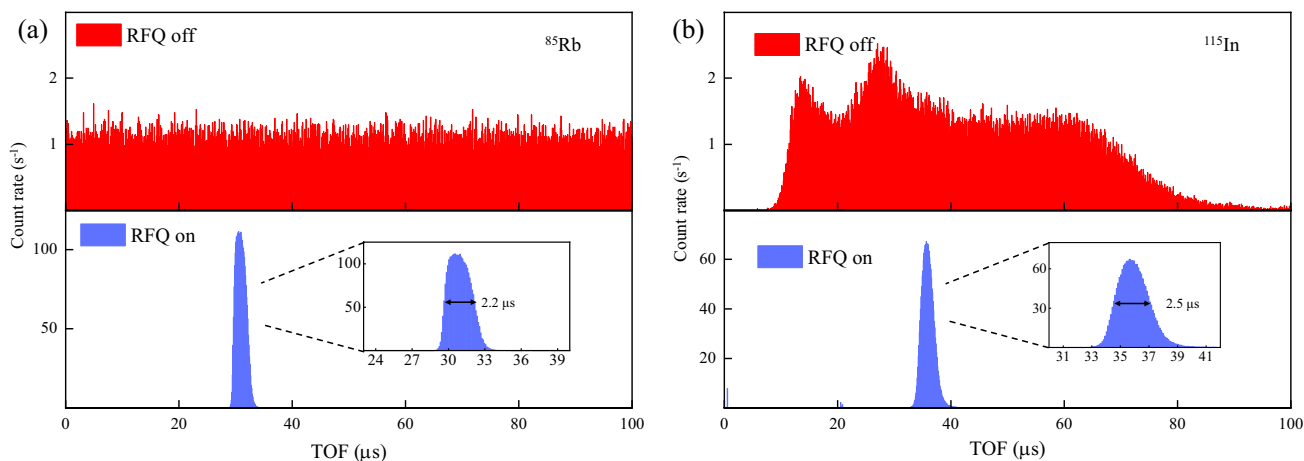
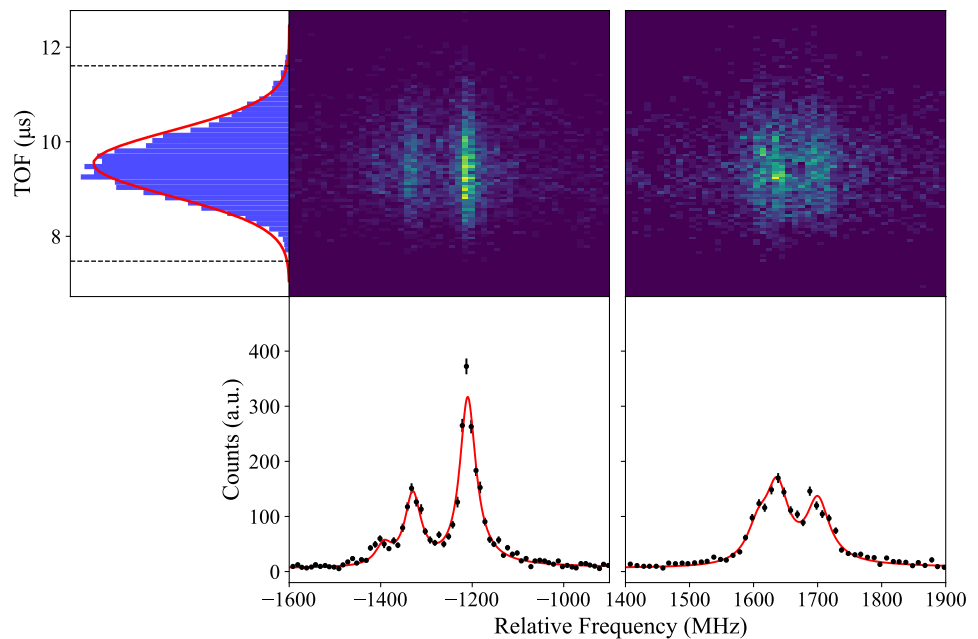


Fig. 5 (Color online) TOF spectra of stable ^{85}Rb and ^{115}In ions detected by the MagneTOF ion detector, with the RFQ cooler-buncher operation off and on. **a** TOF spectra of ^{85}Rb produced from the surface ion source. **b** TOF spectra of ^{115}In produced from the laser ablation ion source

Fig. 6 (Color online) The measured color-coded two-dimensional spectrum of TOF versus frequency for ^{85}Rb (see Ref. [30] for details). The projections onto the x -axis and y -axis correspond to the HFS spectrum and TOF spectrum, respectively



^{38}K , as observed in an earlier experiment [16], the installation of the RFQ cooler-buncher system is crucial not only for producing bunched ion beams but also for reducing the energy spread of the radioactive ion beam. This will undoubtedly enhance the sensitivity and spectral resolution of the planned online collinear resonance ionization laser spectroscopy experiments.

Author contributions All authors contributed to the study conception and design. Material preparation, data collection and analysis were performed by Yin-Shen Liu, Han-Rui Hu, Xiao-Fei Yang, Wen-Cong Mei, Yang-Fan Guo, Zhou Yan, Shao-Jie Chen. The first draft of the manuscript was written by Yin-Shen Liu, Han-Rui Hu, Xiao-Fei Yang and all authors commented on previous versions of the manuscript. All authors read and approved the final manuscript.

Data availability The data that support the findings of this study are openly available in Science Data Bank at <https://cstr.cn/31253.11.sciencedb.j00186.00834> and <https://www.doi.org/10.57760/sciencedb.j00186.00834>.

Declarations

Conflict of interest The authors declare that they have no competing interests.

References

1. Y. Ye, X. Yang, H. Sakurai et al., Physics of exotic nuclei. *Nat. Rev. Phys.* **7**, 21–37 (2025). <https://doi.org/10.1038/s42254-024-00782-5>
2. X. Yang, S. Wang, S. Wilkins et al., Laser spectroscopy for the study of exotic nuclei. *Prog. Part. Nucl. Phys.* **129**, 104005 (2023). <https://doi.org/10.1016/j.pnpnp.2022.104005>
3. T. Yamaguchi, H. Koura, Y. Litvinov et al., Masses of exotic nuclei. *Prog. Part. Nucl. Phys.* **120**, 103882 (2021). <https://doi.org/10.1016/j.pnpnp.2021.103882>
4. C. Ying, Y. Yanlin, W. Kang, Progress and perspective of the research on exotic structures of unstable nuclei. *Nucl. Tech. (in Chinese)* **46**, <https://doi.org/10.11889/j.0253-3219.2023.hjs.46.080020>
5. M.T. Wan, L. Ou, M. Liu et al., Properties of the drip-line nucleus and mass relation of mirror nuclei. *Nucl. Sci. Tech.* **36**, 26 (2025). <https://doi.org/10.1007/s41365-024-01633-9>
6. K. Blaum, J. Dilling, W. Nörtershäuser, Precision atomic physics techniques for nuclear physics with radioactive beams. *Phys. Scr.* **2013**, 014017 (2013). <https://doi.org/10.1088/0031-8949/2013/T152/014017>
7. S. Kaufman, High-resolution laser spectroscopy in fast beams. *Opt. Commun.* **17**, 309–312 (1976). [https://doi.org/10.1016/0030-4018\(76\)90267-4](https://doi.org/10.1016/0030-4018(76)90267-4)
8. W. Nörtershäuser, Recent developments in collinear laser spectroscopy at COLLAPS/SOLDE. *Hyperfine Interact.* **198**, 73–83 (2010). <https://doi.org/10.1007/s10751-010-0230-3>
9. A. Nieminen, P. Campbell, J. Billowes et al., On-line ion cooling and bunching for collinear laser spectroscopy. *Phys. Rev. Lett.* **88**, 094801 (2002). <https://doi.org/10.1103/PhysRevLett.88.094801>
10. A. Vernon, R. de Groote, J. Billowes et al., Optimising the Collinear Resonance Ionisation Spectroscopy (CRIS) experiment at CERN-ISOLDE. *Nucl. Instrum. Methods Phys. Res. Sect. B* **463**, 384–389 (2020). <https://doi.org/10.1016/j.nimb.2019.04.049>
11. R.P. Groote, J. Billowes, C.L. Binnersley et al., Dipole and quadrupole moments of $^{73-78}\text{Cu}$ as a test of the robustness of the $Z=28$ shell closure near ^{78}Ni . *Phys. Rev. C* **96**, 041302 (2017). <https://doi.org/10.1103/PhysRevC.96.041302>
12. G. Alkhazov, L. Batist, A. Bykov et al., Application of a high efficiency selective laser ion source at the IRIS facility. *Nucl. Instrum. Methods Phys. Res. Sect. A* **306**, 400–402 (1991). [https://doi.org/10.1016/0168-9002\(91\)90348-T](https://doi.org/10.1016/0168-9002(91)90348-T)
13. W. Nan, B. Guo, J. Chen et al., Nuclear physics at BRIF. *Prog. Part. Nucl. Phys.* **145**, 104188 (2025). <https://doi.org/10.1016/j.pnpnp.2025.104188>

14. W. Nan, B. Guo, C.J. Lin et al., First proof-of-principle experiment with the post-accelerated isotope separator on-line beam at BRIF: measurement of the angular distribution of $^{23}\text{Na} + ^{40}\text{Ca}$ elastic scattering. *Nucl. Sci. Tech.* **32**, 53 (2021). <https://doi.org/10.1007/s41365-021-00889-9>
15. Q. Wang, X.L. Yan, G.Y. Zhu et al., Precision storage lifetime measurements of highly charged heavy ions in the CSRe storage ring using a Schottky resonator. *Nucl. Sci. Tech.* **36**, 17 (2025). <https://doi.org/10.1007/s41365-024-01614-y>
16. S. Wang, X. Yang, S. Bai et al., Construction and commissioning of the collinear laser spectroscopy system at BRIF. *Nucl. Instrum. Methods Phys. Res. Sect. A* **1032**, 166622 (2022). <https://doi.org/10.1016/j.nima.2022.166622>
17. J. Papuga, PhD Thesis, K. U. Leuven (2015)
18. E. Mané, PhD Thesis, The University of Manchester (2009)
19. K. Minamisono, P. Mantica, A. Klose et al., Commissioning of the collinear laser spectroscopy system in the BECOLA facility at NSCL. *Nucl. Instrum. Methods Phys. Res. Sect. A* **709**, 85–94 (2013). <https://doi.org/10.1016/j.nima.2013.01.038>
20. B. Barquest, J. Bale, J. Dilling et al., Development of a new RFQ beam cooler and buncher for the CANREB project at TRIUMF. *Nucl. Instrum. Methods Phys. Res. Sect. B* **376**, 207–210 (2016). <https://doi.org/10.1016/j.nimb.2016.02.035>
21. E. Mané, J.A. Behr, J. Billowes et al., Collinear laser spectroscopy with reverse-extracted bunched beams at TRIUMF. *Hyperfine Interact.* **199**, 357–363 (2011). <https://doi.org/10.1007/s10751-011-0331-7>
22. C. Kanitz, PhD Thesis, Friedrich-Alexander-University Erlangen-Nürnberg (2021)
23. L. Croquette, PhD Thesis, McGill University (2023)
24. F. Maier, M. Vilen, I. Belosevic et al., Simulation studies of a 30-keV MR-ToF device for highly sensitive collinear laser spectroscopy. *Nucl. Instrum. Methods Phys. Res. Sect. A* **1048**, 167927 (2023). <https://doi.org/10.1016/j.nima.2022.167927>
25. S.W. Bai, X.F. Yang, S.J. Wang et al., Commissioning of a high-resolution collinear laser spectroscopy apparatus with a laser ablation ion source. *Nucl. Sci. Tech.* **33**, 9 (2022). <https://doi.org/10.1007/s41365-022-00992-5>
26. Y.C. Liu, X.F. Yang, S.W. Bai et al., Control and data acquisition system for collinear laser spectroscopy experiments. *Nucl. Sci. Tech.* **34**, 38 (2023). <https://doi.org/10.1007/s41365-023-01197-0>
27. S. Lechner, S. Sels, I. Belosevic et al., Simulations of a cryogenic, buffer-gas filled paul trap for low-emittance ion bunches. *Nucl. Instrum. Methods Phys. Res. Sect. A* **1065**, 169471 (2024). <https://doi.org/10.1016/j.nima.2024.169471>
28. F.G. Major, V.N. Gheorghe, G. Werth, *Charged particle traps: physics and techniques of charged particle field confinement*, vol. 37 (Springer Science and Business Media, Berlin, 2005)
29. P. Zhang, H. Hu, X. Yang et al., Progress in the development of a collinear resonance ionisation laser spectroscopy setup. *Nucl. Instrum. Methods Phys. Res. Sect. B* **541**, 37–41 (2023). <https://doi.org/10.1016/j.nimb.2023.04.020>
30. H.R. Hu, Y.F. Guo, X.F. Yang et al., Development and characterization of a high-resolution, high-sensitivity collinear resonance ionization spectroscopy system. *Science Bulletin* **70**, 2721 (2025). <https://doi.org/10.1016/j.scib.2025.06.036>
31. X.F. Yang, C. Wraith, L. Xie et al., Isomer shift and magnetic moment of the long-lived $1/2^+$ isomer in $^{79}_{30}\text{Zn}_{49}$: Signature of shape coexistence near ^{78}Ni . *Phys. Rev. Lett.* **116**, 182502 (2016). <https://doi.org/10.1103/PhysRevLett.116.182502>
32. K.M. Lynch, J. Billowes, M.L. Bissell et al., Decay-assisted laser spectroscopy of neutron-deficient francium. *Phys. Rev. X* **4**, 011055 (2014). <https://doi.org/10.1103/PhysRevX.4.011055>
33. P. Zhang, PhD Thesis, Peking University (2024)

Springer Nature or its licensor (e.g. a society or other partner) holds exclusive rights to this article under a publishing agreement with the author(s) or other rightsholder(s); author self-archiving of the accepted manuscript version of this article is solely governed by the terms of such publishing agreement and applicable law.